

Characterization and cytocompatibility of hybrid aminosilane-agarose hydrogel scaffolds

V. Sánchez-Vaquero

Departamento de Física Aplicada and Departamento de Biología Molecular, Universidad Autónoma de Madrid and Centro de Investigaciones Biomédicas en Red, Bioingeniería, Biomateriales y Nanomedicina (CIBER-BBN), 28049 Madrid, Spain

C. Satriano

Dipartimento di Chimica, Università degli Studi di Catania, V. le Andrea Doria, 6, 95125 Catania, Italy

N. Tejera-Sánchez, L. González Méndez, J. P. García Ruiz, and M. Manso Silván^{a)}

Departamento de Física Aplicada and Departamento de Biología Molecular, Universidad Autónoma de Madrid, 28049 Madrid, Spain and Centro de Investigaciones Biomédicas en Red, Bioingeniería, Biomateriales y Nanomedicina (CIBER-BBN), 50018 Zaragoza, Spain

(Received 11 February 2010; accepted 17 March 2010; published 21 April 2010)

Agarose hydrogels containing aminopropyl triethoxy silane (APTS) have been prepared and evaluated as scaffolds for adhesion and proliferation of human mesenchymal stem cells (hMSCs). The preparation of the hydrogels involved the conventional melting of agarose in water followed by addition of APTS as functional group carrier. The resulting hydrogel supports have been studied by Fourier transformed infrared spectroscopy in order to get an insight into the hybrid molecular structure. X-ray photoelectron spectroscopy has been used for the analysis of the surface chemical composition of the hydrogels. It is deduced from these data that the resulting hybrid structure presents two phases with a clear tendency toward APTS surface segregation. Moreover, the observation of the desiccated hydrogel surfaces by atomic force microscopy shows that the films acquire a filament-mesh structure for increasing APTS content, while the pure agarose supports exhibit a granular structure. As a result of such a structure, the hydrogel surfaces show a hydrophobic behavior, as determined by water contact angle measurements. The biocompatibility of such platforms is supported by adhesion-proliferation assays performed with hMSCs. It is concluded that although adhesion is lower on APTS rich scaffolds, the proliferation rate on these surfaces is higher so that total number of proliferating cells does not significantly depend on APTS content in the hydrogels. © 2010 American Vacuum Society. [DOI: 10.1116/1.3388182]

I. INTRODUCTION

Traditional hydrogels are currently a continuous resource for the production of combinatorial biomaterials with adapted response to different cellular or tissue environments. In particular, hybrid hydrogels can be designed to resemble extracellular matrix (ECM), which includes all secreted molecules that are immobilized outside the cells. First advances in hydrogel-based hybrid biomaterials were related to the development of *in vitro* autologous cell implants.¹ Since then, hydrogels have contributed to composite materials with their intrinsic hydrophilic properties and reputed biocompatibility. With these ingredients, hybrid hydrogels of different origins have been designed to promote cell proliferation in three-dimensional porous scaffolds,^{2,3} to form stamps for the transfer of cells onto surfaces,⁴ to encapsulate cells in hydrated environments,^{5,6} and to deliver transforming growth or differentiation factors.^{7,8} Paradox examples exist in which the hydrogel structures are used to control the surface tension of the combined material with a superhydrophobic behavior.⁹ In particular, the functionality of loaded factors and other

biomolecules can be controlled in the structure by tuning ambient charge conditions.²

Natural hybrid hydrogels in ECM include collagens and noncollagenous glycoproteins [proteins that are post-translationally modified with glycosaminoglycan (GAG) polysaccharides]. There are many proteins that bind GAG such as laminin,¹⁰ which plays a fundamental role in tissue repair at the neuromuscular junctions. Moreover, plants and algae produce relevant hydrogels as alginate,^{1,5} agarose,² and methylcellulose,^{9,11,12} which emerge as preferred nonamine polysaccharides for hybrid biomaterial design.

Hydrogel hybrids with bioinorganic materials, such as composites with silanes,¹³ hydroxyapatite,^{14–16} and other calcium phosphates^{17,18} have been already described. In several cases, the formation of the hybrids includes ternary combinations of the above cited structures.¹⁹ The intimate contact between the different integrants of the hybrid varies in a wide spectrum of possibilities. While certain polysaccharides form hybrid hydrogels by spontaneous ramification,²⁰ the formation of complex structures often requires photoinduced,²¹ chemical,^{2,9} or biochemical enzymatic cross-linking²² routes to form the designed conjugates.

It is of note that hybrid hydrogel materials have found applications in mimicking a wide spectrum of tissues. For

^{a)}Author to whom correspondence should be addressed; electronic mail: miguel.manso@uam.es

instance, they have been mainly designed for the regeneration of different lineages of mesenchymal tissues by optimizing with hybrid hydrogels the growth, proliferation, and differentiation of mesenchymal stem cells (MSCs). Studies have been performed in bone^{8,14,18,19,23} cartilage¹ and ligament.²⁴ The possibility to comply simultaneously with the requirements of two osteochondral tissues has been outlined by forming layered²⁵ and graded¹⁷ hybrid structures that fulfill a bone-inducing structure on one side and a cartilage-inducing structure on the other.

The present work aims at the formation and characterization of hybrids based on agarose and the organometallic 3-aminopropyl-triethoxysilane (APTS), a common biofunctionalizing molecule already transferred to silicon substrates from such hybrid hydrogels.²⁶ It has been shown previously that APTS can induce surface modifications, which influence through engineered^{27,28} or spontaneous²⁹ protein adsorption the behavior of cultured MSCs. The effects of APTS modification in the properties of agarose scaffolds for MSCs are the focus of this study.

II. EXPERIMENT

A. Hybrid hydrogel preparation

Agarose hydrogels (ultrapure electrophoresis grade, Gibco BRL) were prepared by melting in milli-*Q* water (18 k Ω cm) at 90 °C and concentrations of 5 wt %. APTS (Purum 96%, Fluka) was added in aliquots so as to maintain a proportional weight ratio with respect to agarose (i.e., APTS wt %/agarose wt % = 1, 2, and 4). Flat homogeneous agarose/APTS hydrogels were prepared onto the (100) silicon (1 \times 1 cm²) by cooling down from 90° until jellification in room conditions. Control surfaces with a self-assembled APTS film were prepared for surface analysis [x-ray photoelectron spectroscopy (XPS), water contact angle (wCA) measurements] as previously detailed.²⁶ Briefly, Si (100) substrates were immersed in a piranha solution (4:1, H₂SO₄:H₂O₂), rinsed in de-ionized water and toluene, immersed in a 0.2% solution of APTS in dry toluene, and doubly rinsed in dry toluene.

B. Hydrogel characterization

For the characterization of the hybrid hydrogels by Fourier transformed infrared (FTIR) spectroscopy, films were prepared by spinning at 2000 rpm onto flat, double side polished Si (100) substrates. The FTIR characterization was performed in transmission mode under vacuum conditions by using a Bruker Vector 22 (resolution 8 cm⁻¹, 4000–400 cm⁻¹, and 32 scans at 10 KHz).

XPS measurements were performed at a base pressure of 2 \times 10⁻⁹ torr by using a PhiEsca/Sam 5600 Multy technique spectrometer, with a standard Al *K* α radiation source. The operating conditions were kept constant at 14 keV and 300 W, with an emission current of 30 mA. Spectra were recorded with an instrumental resolution <0.4 eV. The XPS binding energy (BE) scale was calibrated by centering the C

1s peak of the adventitious carbon at 285.0 eV. The XPS peak intensities were obtained after Shirley background removal.

Atomic force microscopy (AFM) (Multimode Nanoscope IIIA, Veeco) was operated in tapping mode in air with a standard phosphorus (*n*) doped silicon tip, having a nominal constant force of 20–80 N/m. Modification of the surface wettability was traced by measuring dynamic and static wCAs along periods of 5 min onto transferred films dried overnight. Drying and measurements were carried out in controlled atmosphere (25 °C and 65% relative humidity) with an OCA30 instrument (Dataphysics). Probe liquid drops of 2 μ l of volume were applied on different zones of each sample surface and by digital image analysis the static contact angles were measured on both sides of the two-dimensional projection of the droplet. At least five measurements were made for each sample and then averaged.

C. MSCs culture

Human MSCs (hMSCs) from bone marrow were used and their patterns followed onto the hybrid materials. The cells were isolated from bone marrow and the culture expansion was carried out as previously described.³⁰ The biocompatibility of the agarose-APTS supports was assayed by adhesion and proliferation studies. About 15 000 cells were seeded on each sample (1 cm²) after rehydration with phosphate by buffer saline (PBS) and Dulbecco's modified Eagle's medium with low glucose (DMEM-LG). Cells were incubated on the materials with DMEM-LG including 10% fetal bovine serum (FBS) during 72 h at 37 °C in 5% CO₂. Then, the cells were washed with PBS and fixed in 3.7% formaldehyde in PBS for 15 min at RT. In order to analyze the cytoskeleton and nuclei, cells were permeated in 0.1% Triton X-100 in PBS to favor antibody and staining reactions. After washing, the surfaces were incubated in dark conditions for 1 h with fluorescent conjugates: DNA in nuclei was labeled with 4',6-diamidino-2-phenylindole (DAPI) (blue) and actin cytoskeleton with phalloidin (green). Monoclonal antirabbit Ki67 (red) was further used as immunocytochemical indicator of proliferation activity in the nucleus. After incubation, the cells were visualized in an Olympus fluorescence inverted microscope coupled to a charge coupled device color camera. For statistical analysis, cellular assays were performed with four different replicas and images were obtained from four different areas of each surface. Quantitative analysis was performed using OLYMPUS software.

III. RESULTS

A. FTIR characterization

The modifications induced by the integration of APTS in the agarose hydrogels were initially analyzed by FTIR spectroscopy. Figure 1 depicts the spectra corresponding to different molecular ratios between the polysaccharide and the aminosilane. All the spectra matched the pattern of bands corresponding to agarose³¹ with main bands in the range of

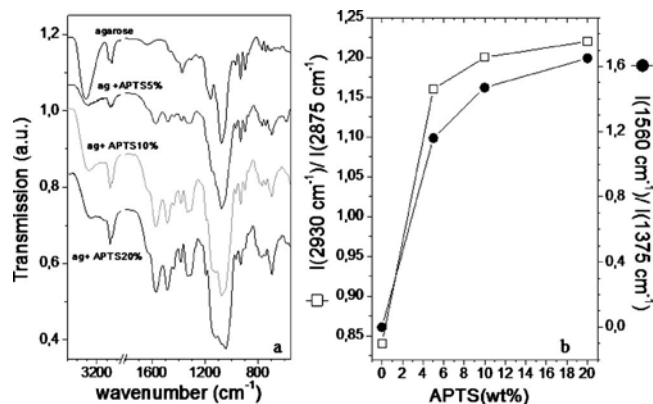


FIG. 1. FTIR spectra from reference agarose and APTS doped agarose gels (a). Plot of ratios between bands at 2930 and 2875 cm^{-1} (corresponding to CH_3 and CH_2 , respectively) and 1560 and 1375 cm^{-1} (corresponding to C—O—C and NH_2 , respectively) (b).

3600–2900 cm^{-1} (assigned to OH and CH_x), characteristic water adsorption at 1650 cm^{-1} , vibrations at around 1100, 930, and 890 cm^{-1} , a sharp absorption at 1375 cm^{-1} (characteristic of C—O—C), and a very low intensity band at 1250 cm^{-1} indicating the presence of sulfate groups in the reference agarose. However, the incorporation of the silane in the hydrogel structure induces clear effects as complementary bands around 1100–1200 cm^{-1} . In particular, the new band at 1125 cm^{-1} , assigned to symmetric stretch of Si—O—C structures, is a trace mark for poorly condensed alkoxy silane structures.³² In our case, this increasing band hides the originally well resolved two component band of the agarose spectrum. Other scaled modifications can be observed in the increasing background band at 790 cm^{-1} (assigned to Si—C rocking). The presence of this band is of relevance since it proves that the nonhydrolysable Si-aminopropyl bond is stable and remains active in the hybrid structures.²⁹ Furthermore, the emerging midintensity bands at 1320 and 1560 cm^{-1} (assigned to wagging NH_2) overcome the intensity of the agarose C—O—C mode at 1375 cm^{-1} , thus providing a direct label of amino functionalization in the combined hydrogels. Moreover, the modified ratio between the double band at 2875 and 2930 cm^{-1} (assigned to stretching vibration modes of CH_3 and CH_2 , respectively), which appears reversed already at the lowest APTS concentrations added, is another indication of the gradual modification. The ratios between these bands [plotted in Fig. 1(b)] illustrate a tendency toward saturation. Finally, also the increased background around 3300 cm^{-1} due to NH_2 symmetric and asymmetric stretching reflects a gradually modified chemistry in the hybrid gels.

As an overview of FTIR results, the spectra show that incorporation in the agarose gel of the aminopropyl bond of APTS is possible due to the hydrolysis resistant Si—C bond in APTS. This fact is further illustrated by the direct detection of the primary amine bands. However, there is no evidence of the presence of new molecular structures formed upon reaction of agarose with APTS so that networks formed appear to be relatively independent.

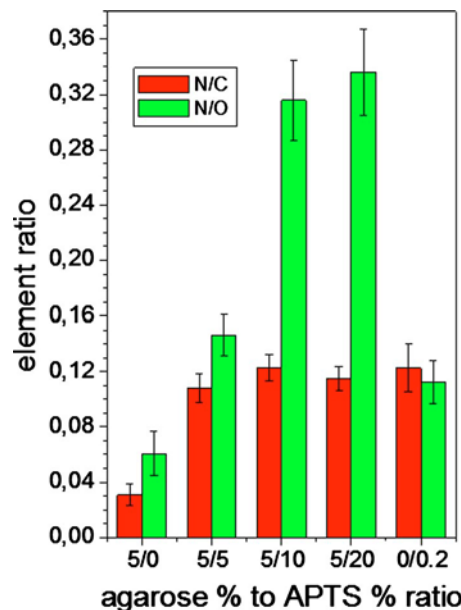


FIG. 2. (Color online) Relative N composition with respect to C and O as derived from survey spectra for increasing APTS incorporation in the agarose hydrogel [0/0.2 corresponds to an APTS self-assembled film on Si (100)].

B. XPS characterization

An initial study was devoted to the determination of elemental composition of hybrid hydrogel from the survey spectra analysis. Carbon and oxygen are the principal chemical constituents of all the hybrid hydrogel films, followed by silicon (except for 100% agarose where it was not observed). Finally, evidence of nitrogen, which can be taken as the XPS marker of the APTS presence, appeared notably in all the hybrid APTS-hydrogel samples, while small amounts of trace elements (F and S) were also detected in particular samples. A clear tendency toward higher N atomic content with respect to C and O was observed for increasing integration of APTS in the agarose network (histograms in Fig. 2). Furthermore, the trend of the N/C ratio indicates that the N composition can be increased up to a saturation value (i.e., around 0.12), in coincidence with the experimental value obtained for the self-assembled APTS control (see 0/0.2 columns in Fig. 2). This finding evidences the clear tendency of APTS to occupy preferentially surface positions with respect to the agarose network in the hybrid system. The increasing trend of the N/O ratio observed until values of 20% by weight of APTS reflects a clearly lower O content with respect to the control self-assembled sample. It should be underlined that for the control self-assembly [ideally only 1 ML (monolayer)] there is also a contribution from the underlying hydroxylated silicon (SiO_x), which accounts for the increased O composition. In overall, by taking into account the theoretical stoichiometry of the APTS molecule ($\text{N/C}=0.11$, $\text{N/O}=0.33$, and $\text{C/O}=3$), our results indicate that the surface of hybrid hydrogels has reached an APTS composition close to saturation already at 10% APTS integration (N/C

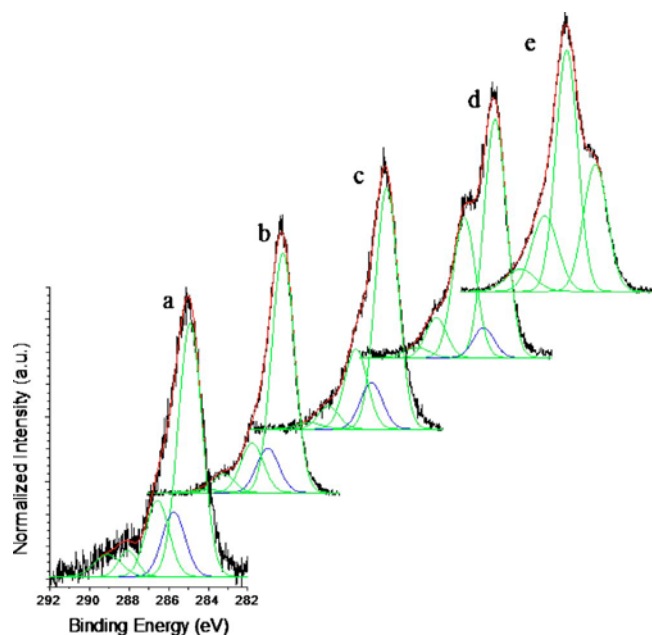


FIG. 3. (Color online) C 1s high resolution spectra for an APTS self-assembled layer (a) and for the APTS containing agarose hydrogels: 20% (b), 10% (c), 5% (d), and 0% (e) APTS contents.

=0.12, N/O=0.31, and C/O=2.57) and even closer at 20% APTS composition (N/C=0.11, N/O=0.33, and C/O=2.92).

Next steps of the characterization were devoted to the analysis of the C 1s and N 1s core level spectra related to the amino functionalization group. Figure 3 presents a set of C 1s spectra corresponding to the reference sample of self-assembled APTS [spectrum (a)], to hybrid APTS-agarose hydrogels containing decreasing APTS fractions [spectra (b)–(d)], and to the reference sample of pure agarose hydrogel [spectrum (e)]. The spectra corresponding to the hybrid hydrogels have been deconvoluted with a model taking into account five contributions corresponding to (1) C—C from the propyl chain in APTS (BE=284.5 eV), (2) C—N (BE=285.4 eV) from amino groups specific to the APTS containing hydrogels, (3) O—C (BE=286.4 eV) from the agarose backbone and poorly condensed alkoxy groups in APTS, (4) O—C—O (BE=288.0 eV) in the agarose backbone, and (5) carboxyl O=C—O (BE=288.9 eV) plausibly bound from CO₂ adsorption and degradation of amines through urea formation, respectively.

The comparison of the APTS containing hydrogels with the APTS reference sample [Fig. 3(a)] shows that the C—H component is the dominant surface structure, which is in agreement with a preferential exposure of APTS to the surface of the hybrid materials [Figs. 3(b)–3(d)]. On the other hand, the reference agarose sample [Fig. 3(e)] presents a C—O principal component, which also appears as an intense shoulder in the hybrid sample with lowest APTS integration [5% APTS, Fig. 3(d)]. The peak deconvolution evidences that this C—O contribution decreases in intensity as the APTS load in the structure increases.

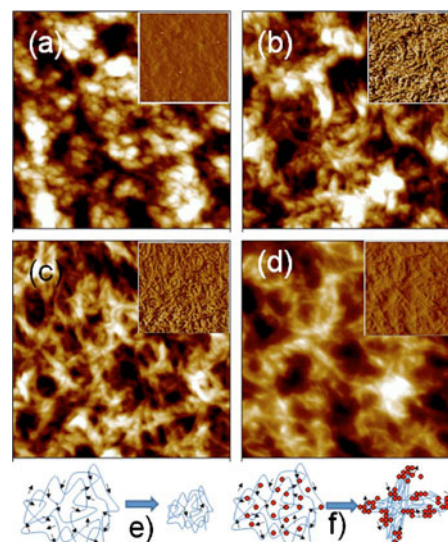


FIG. 4. (Color online) AFM images ($1 \times 1 \mu\text{m}^2$) from the surfaces of desiccated hydrogels agarose 100% (a), ag+ APTS 5% (b), ag+ APTS 10% (c), and ag+ APTS 20% (d). $x=y=1 \mu\text{m}$ and $z=20 \text{ nm}$. Schematic representation of hydrogel structure after dehydration for pure agarose (e) and hybrid agarose-APTS (f).

It is also worth noting the absence of the amino related C—N bond contribution in the pure agarose hydrogel [note outlined darker contribution in the (a)–(d) spectra in Fig. 3]. There is furthermore a surprising agreement between the relative intensity of the C—O and C—N contributions for the hybrid hydrogel sample with highest (20%) APTS integration and the APTS self-assembled monolayer. This result reinforces the idea of the possibility to saturate the agarose surface with APTS by loading this precursor at 20%.

The analysis of the N 1s core level spectra corresponding to hybrid samples (not shown) has been performed according to a model consisting in two contributions. These can be ascribed to neutral (BE=400.0 eV) and positively charged (BE=401.5 eV) amino groups, respectively, although it has been already reported that the lower BE peak may be also associated to a degradation of the amino group by C=O bonding,³³ which suggests that hybrid hydrogels may suffer from atmospheric degradation.

C. Surface morphology

The surfaces of the hybrid hydrogels were explored after drying at room temperature by using AFM in order to get an insight to the surface micronanostructure. Figure 4 includes the topography and phase images of the agarose reference and the APTS loaded agarose samples with increasing APTS (5%, 10%, and 20%). All the samples present irregular surfaces with several blind areas suggesting the presence of a nanoporous structure. A gradual change from an agglomerated nanosphere environment as observed for non-APTS containing hydrogels [see Fig. 4(a)] toward a dendritic filament mesh, observed for APTS rich hydrogels is visible [see specially Fig. 4(d)]. This tendency toward a filamentary morphology is also clearly visible in the corresponding phase

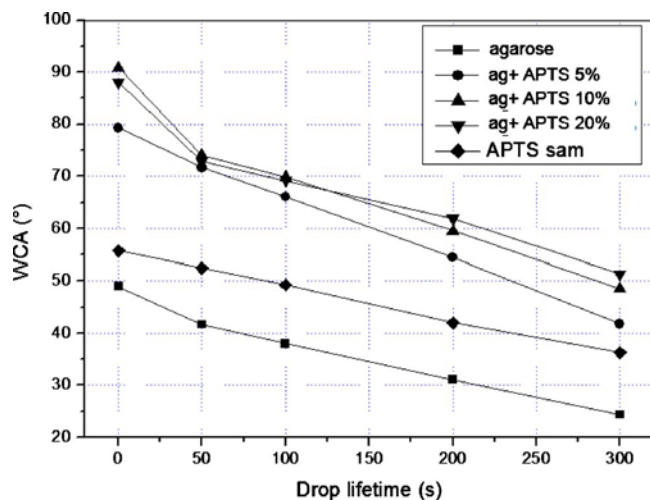


FIG. 5. (Color online) Evolution of wCA onto desiccated agarose-APTS hybrid hydrogels.

images [see insets in Figs. 4(a)–4(d)]. Furthermore, the width of the filament structures formed reduces for increasing APTS content. It is worth to note that the modification of the surface decoration was accompanied by an alteration of characteristic values of surface roughness. In fact, the tendency of these values from 6.3 ± 0.3 nm for the pure agarose hydrogel to 5.3 ± 0.5 nm for the 20% APTS containing hydrogel reflects a certain capacity of APTS to compress the hydrogel upon drying. At this point, it is worth mentioning that APTS presents a tendency toward formation of nanocolloids in water solutions and subsequent agglomeration upon drying.^{26,34} The driving force for the filament microstructure observed in hybrid hydrogels would mostly arise from the formation and aggregation of APTS nanocolloids. Furthermore, the morphology is also influenced by final content of adsorbed water and the kinetics of drying. A final factor influencing the morphology is the preferential surface presence of the APTS (as suggested by XPS characterization) suggesting that it could act as a confining network during drying condensation. Figures 4(e) and 4(f) illustrate schematically the processes leading to the final microstructures observed for pure agarose and hybrid agarose-APTS hydrogels, respectively.

D. wCA onto desiccated hydrogels

The hydrophobic-hydrophilic character of the formed hydrogels was determined by measuring wCAs and following the interaction kinetics between the water microdrops and the samples during 5 min. Results of measurements on the hybrid materials and two reference controls, i.e., the 100% agarose film and the APTS self-assembled monolayer on silicon, are presented in Fig. 5. It is evident that agarose is the most hydrophilic substrate compared to the surface immobilized APTS hydrogels. Surprisingly, the hybrid materials showed a more hydrophobic behavior than the reference APTS surface. Within the molecular ranges studied, the increase in APTS increases the wCA but a saturation value is

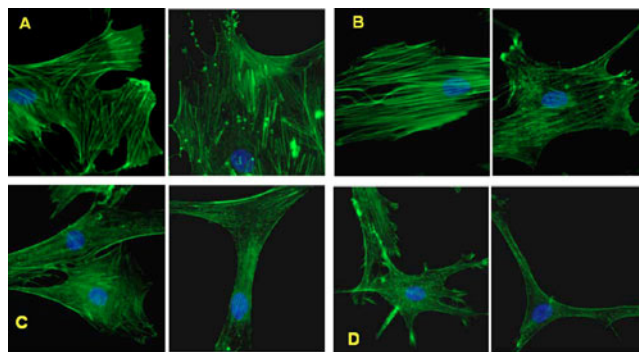


FIG. 6. (Color online) Fluorescence microscopy images after double staining of hMSCs cultured on hybrid scaffolds with increasing APTS content: agarose (a), ag+ APTS 5% (b), ag+ APTS 10% (c), and ag+ APTS 20% (d).

reached at approximately 10% APTS in view of the similar trend, as compared with 20% APTS hybrid hydrogels.

With respect to the wetting kinetics, it can be observed that during the 50 first seconds, the agarose containing surfaces suffer a faster decrease in wCA as if a surface swelling process was taking place. This initial swelling process is even faster for APTS rich hybrid hydrogels. For the rest of the time studied, the wCA receding velocity is similar among the hybrid samples and among the control samples, respectively. The comparison of these results with topographic AFM images supports the idea that there may be strong morphological aspects influencing the wettability behavior of the surfaces. In particular, the filament structures in APTS containing hydrogels may act as a pit structure introducing bubbles and inducing a more hydrophobic behavior. For instance, in terms of previous models for hydrophobic behavior of hydrogels,³⁵ the filament structures could introduce a considerable increase in surface area with respect to the agarose surface and lead, in cooperation with chemical changes, to the formation of a more hydrophobic surface.

E. Cell adhesion and proliferation

The culture of hMSCs on the surfaces of agarose and hybrid agarose hydrogels was analyzed after double staining by fluorescence microscopy. The results regarding surface morphology and adhesion after 72 h of culture are presented in Fig. 6. The control agarose surfaces induced an intense adhesion of hMSCs that extended occupying larger surface areas [Fig. 6(a), 1800 ± 400 μm^2] than cells cultured onto the hybrid hydrogel surfaces (1200 ± 300 , 650 ± 100 , and 360 ± 70 μm^2 for increasing APTS content, respectively). It is thus of note that by increasing the APTS content in the hybrid materials, the surface area occupied by the cells diminished notably but the capacity to form filopodia increased dramatically [Figs. 6(b) and 6(c)]. In fact, at the highest APTS concentrations used, the hMSCs showed characteristic striated forms with formation of dendritic actin structures as eccentric focal adhesions.

In order to define the best surfaces for proliferative purposes, a quantitative analysis was performed in order to establish the number of cells per unit area for each type of

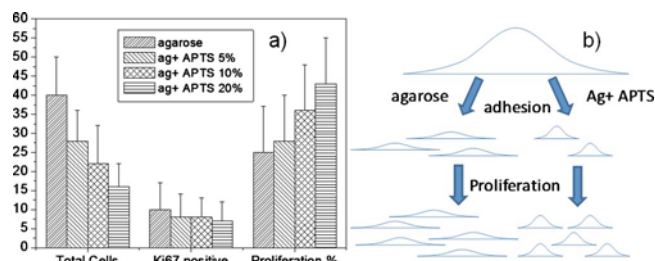


FIG. 7. (Color online) Statistics of surface adhesion, proliferation (mean values per area of 0.056 mm^2), and relative proliferation histograms after culture of hMSCs on the hybrid scaffolds (a). Schematic representation of paths followed by hMSCs upon adhesion on agarose and hybrid agarose-APTS hydrogels (b).

support as well as the fraction of cells with proliferative activity, as revealed by Ki67. The results of this additional study are presented in the histogram in Fig. 7(a) and relate to areas of 0.056 mm^2 . The first set of columns of the figure indicates clearly that the reference supports of pure agarose behave as ideal substrates for fast cell adhesion, while the hybrid hydrogels exhibit a diminution of adhesion for increasing APTS load. The second set of columns, reporting the number of Ki67 positive cells for each kind of surface, evidences a very similar behavior for all surfaces. However, taking into account the fraction of cells with respect to adhered population, the cells on the APTS rich surfaces present higher proliferative rates, as denoted in the third set of columns in Fig. 7(a).

IV. DISCUSSION

The analysis of the formation of hybrid agarose-APTS hydrogels has shown that the hybrids are constituted by two relatively independent networks as confirmed by FTIR results and as previously described by magic angle spinning nuclear magnetic resonance.²⁶ The use of these surfaces as tissue engineering scaffolds requires a deep analysis of the surface properties. Composition analysis shows that introduction of APTS in the agarose network changes dramatically the surface composition. The XPS analysis evidenced the increase of C and N elemental composition, which is correlated with the increase in C—C and C—N bonding in C 1s core level spectra. Such a finding suggests the preferential orientation of aminopropyl groups toward the surface, which in turn induces collateral morphologic and surface tension modifications. AFM measurements evidenced that the surfaces of APTS enriched hydrogels exhibit upon drying a filament distribution in contrast with the agarose initial spherical mesh morphology. Increasing APTS induces narrower filament structures. These morphological changes are considered to be responsible for the increased hydrophobic character of the hydrogels at increasing APTS content, as measured by wCA measurements. In fact, the formation of thinner filamentary structures for increasing APTS composition may be responsible for a drastic increase in specific

surface area conducting to an increasing hydrophobic character, the measured wCA being even higher than that for the reference surfaces of pure APTS

These above described physic-chemical properties of the hybrid APTS-agarose hydrogel films are in turn responsible of a graded behavior of hMSCs toward both adhesion and proliferation. In fact, the total number of adhered cells decreases and the rate of proliferating cells increases as the APTS content in the hybrids increases. Therefore the density of proliferative cells is estimated significantly comparable for all supports. These phenomenological features (cell areas, adhesion, and population of proliferative cells) are illustrated in the schematic of Fig. 7(b). These results may be interpreted in terms of the presence of two surface barrier potentials, one toward adhesion and another toward proliferation. These are inherently linked since adhesion is a *sine qua non* condition for proliferation. The first of these barriers would be higher for increasing APTS containing supports but the second barrier would behave on the opposite way giving higher rates of proliferating hMSCs for increasing APTS. The increasing hydrophobic character may orientate adhesion receptors and membrane protein molecules and be responsible for proliferation enhancement. However, a surface charge positive potential induced by amine groups in APTS may play an important role in these aspects. In fact, the morphological stage of proliferating hMSCs in previously studied positively charged APTS rich supports consisted in a tendency to filopodia extension.³² However, no direct evidence, such as chemical signaling pathways, has been established between the capacity of hMSCs to form strong eccentric focal adhesions and their proliferation stage.

V. CONCLUSIONS

Hybrid agarose-APTS hydrogels can be prepared by a conventional agarose melting in water and final mixing with different APTS aliquots. The hybrid hydrogels are composed of two independent networks in which APTS tends to occupy the surface. These macromolecular organization gives rise to APTS controlled properties and determines surface composition, morphology, and wettability of the surfaces. The behavior of hMSCs on these surfaces toward adhesion and proliferation can be understood in terms of a double surface barrier potential related to APTS content on the hybrid materials. The higher the APTS concentration, the lower the rate of adhered cells but the higher the rate of proliferating cells and vice versa. Although direct evidence is not yet available, the increasing hydrophobic properties or surface positive charge at increasing APTS composition are pointed out as possible mechanisms responsible for the presence of surface barrier potentials for cell adhesion and proliferation. Comparison of these results in similar systems as well as biochemical analysis of signaling pathways potentially expressed upon adsorption on APTS doped materials is required in order to establish a behavioral pattern for hMSCs.

ACKNOWLEDGMENTS

The authors are especially thankful to L. García Pelayo for his technical assistance during polymer processing and characterization. This research was partially funded by the FEDER through CIBERbbn.

- ¹Y. L. Cao, A. Rodriguez, M. Vacanti, C. Ibarra, C. Arevalo, and C. A. Vacanti, *J. Biomater. Sci., Polym. Ed.* **9**, 475 (1998).
- ²G. P. Dillon, X. J. Yu, A. Sridharan, J. P. Ranieri, and R. V. J. Bellamkonda, *Biomater. Sci., Polym. Ed.* **9**, 1049 (1998).
- ³F. Tortelli and R. Cancedda, *Eur. Cells Mater* **17**, 1 (2009).
- ⁴M. M. Stevens, M. Mayer, D. G. Anderson, D. B. Weibel, G. M. Whitesides, and R. Langer, *Biomaterials* **26**, 7636 (2005).
- ⁵G. D. Nicodemus and S. J. Bryant, *Tissue Engin. B* **14**, 149 (2008).
- ⁶S. J. Lee, T. Kang, J. W. Rhie, and D. W. Cho, *Sens. Mater.* **19**, 445 (2007).
- ⁷C. R. Nuttelman, D. J. Mortisen, S. M. Henry, and K. S. Anseth, *J. Biomed. Mater. Res.* **57**, 217 (2001).
- ⁸J. C. Tong and S. L. Yao, *J. Bioact. Compat. Polym.* **22**, 232 (2007).
- ⁹G. Zhang, D. Wang, Z. Z. Gu, and H. Mohwald, *Langmuir* **21**, 9143 (2005).
- ¹⁰S. E. Stabenfeldt, A. J. Garcia, and M. C. LaPlaca, *J. Biomed. Mater. Res. Part A* **77A**, 718 (2006).
- ¹¹M. C. Tate, D. A. Shear, S. W. Hoffman, D. G. Stein, and M. C. LaPlaca, *Biomaterials* **22**, 1113 (2001).
- ¹²C. Vinatier *et al.*, *J. Biomed. Mater. Res. Part A* **80A**, 66 (2007).
- ¹³A. Costantini, G. Luciani, B. Silvestri, F. Tescione, and F. Branda, *J. Biomed. Mater. Res., Part B: Appl. Biomater.* **86B**, 98 (2008).
- ¹⁴M. A. Bokhari, G. Akay, S. G. Zhang, and M. A. Birch, *Biomaterials* **26**, 5198 (2005).
- ¹⁵C. P. Huang, X. M. Chen, and Z. Q. Chen, *Mater. Lett.* **62**, 1499 (2008).
- ¹⁶C. Tsiptsias, I. Tsivintzelis, L. Papadopoulou, and C. Pallayiotou, *Mater. Sci. Eng., C* **29**, 159 (2009).
- ¹⁷T. Taguchi, Y. Sawabe, H. Kobayashi, Y. Moriyoshi, K. Kataoka, and J. Tanaka, *Mater. Sci. Eng., C* **24**, 881 (2004).
- ¹⁸M. D. Weir, H. H. K. Xu, and C. G. Simon, *J. Biomed. Mater. Res. Part A* **77A**, 487 (2006).
- ¹⁹M. Endres *et al.*, *Tissue Eng.* **9**, 689 (2003).
- ²⁰H. P. Tan, C. R. Chu, K. A. Payne, and K. G. Marra, *Biomaterials* **30**, 2499 (2009).
- ²¹S. A. Zawko, S. Suri, Q. Truong, and C. E. Schmidt, *Acta Biomater.* **5**, 14 (2009).
- ²²C. W. Yung, L. Q. Wu, J. A. Tullman, G. F. Payne, W. E. Bentley, and T. A. Barbari, *J. Biomed. Mater. Res. Part A* **83A**, 1039 (2007).
- ²³K. Hamada, M. Hirose, T. Yamashita, and H. Ohgushil, *J. Biomed. Mater. Res. Part A* **84A**, 128 (2008).
- ²⁴M. Bosetti, F. Boccafocchi, A. Calarco, M. Leigheb, S. Gatti, V. Piffanelli, G. Peluso, and M. Cannas, *J. Biomater. Sci., Polym. Ed.* **19**, 1111 (2008).
- ²⁵L. Liu, Z. Xiong, R. J. Zhang, L. Jin, and Y. N. Yan, *J. Bioact. Compat. Polym.* **24**, 18 (2009).
- ²⁶M. Manso Silván, G. M. L. Messina, I. Montero, C. Satriano, J. P. García Ruiz, and G. Marletta, *J. Mater. Chem.* **19**, 5226 (2009).
- ²⁷R. Müller *et al.*, *Biomaterials* **26**, 6962 (2005).
- ²⁸M. C. Porté-Durrieu *et al.*, *Biomaterials* **25**, 4837 (2004).
- ²⁹M. Manso Silván *et al.*, *J. Biomed. Mater. Res. Part B: Appl. Biomater.* **83B**, 232 (2007).
- ³⁰D. P. Lennon, S. E. Haynesworth, S. P. Bruder, N. Jaiswal, and A. I. Caplan, *In Vitro Cell. Dev. Biol.: Anim.* **32**, 602 (1996).
- ³¹J. C. Mollet, A. Rahaoui, and Y. Lemoine, *J. Appl. Phys.* **10**, 59 (1998).
- ³²M. Arroyo-Hernández, M. Manso-Silvan, E. Lopez-Elvira, A. Muñoz, A. Climent, and J. M. Martínez Duart, *Biosens. Bioelectron.* **22**, 2786 (2007).
- ³³C. Perruchot, J. F. Watts, C. Lowe, R. G. White, and P. J. Cumpson, *Surf. Interface Anal.* **33**, 869 (2002).
- ³⁴T. Leichlé *et al.*, *Nanotechnology* **16**, 525 (2005).
- ³⁵K. Haraguchi, H. J. Li, and L. Song, *J. Colloid Interface Sci.* **326**, 41 (2008).